small structures
www.small-structures.com

Recent Progress in Ionic Liquids for Stability Engineering of Perovskite Solar Cells

Fei Wang, Chuang-ye Ge, Dawei Duan, Haoran Lin, Liang Li, Pančе Naumov,* and Hanlin Hu**

Perovskite solar cells attract widespread attention due to their impressive power conversion efficiencies, high absorption coefficients, tunable bandgap, and straightforward manufacturing protocols. However, in the process of further development and optimization toward mass production, the long-term stability stands as one of the most urgent challenges that need to be overcome. Given the excellent thermal stability and high structural designability, ionic liquids (ILs) are relatively green room-temperature molten salts that have been widely applied to perovskite photovoltaic devices with promising results in view of improved stability and enhanced device performance. In this review, the reasons and mechanisms of instability of such devices under external and internal factors are analyzed. The current strategies of ILs engineering for improved stability of the devices are classified and summarized, including the IL-assisted perovskite film evolution and IL-modified photophysical properties of the perovskite photoactive layer and the related stability and photovoltaic performance of the devices. The challenges that stand as obstacles toward further development of perovskite solar cells based on IL engineering and their prospects are also discussed.

1. Introduction

A historic breakthrough has been made with the increased efficiency of perovskite solar cells (PSCs) from 3% to 25.7% in the recent years.[1–3] Based on these unprecedented power conversion efficiencies (PCEs), as well as due to the simple production process and tunable bandgap, the field of PSCs has attracted the attention of a sizeable research community.[4–6] Through continuous control over the device processing and structure, the PSCs are now commonly regarded as the most promising candidates for the next-generation photovoltaic devices.[6,7] Taking the advantages of the potential for practical applications, the researchers' focus has shifted to efficient PSCs with long operational lifetime that would respond to the commercial demand.[8,9]

However, the operational lifetime depends on the stability of the PSCs, which is affected by both external and intrinsic factors. Poor stability caused by these factors will inevitably lead to a significant decline in the performance of the device, thereby hindering further development of such devices. The external factors mainly include the impact of the external environment such as oxygen, temperature, and humidity. The instability caused by these external factors can usually be improved by using different packaging processes and/or materials.[10] Therefore, as the primary factor that determines the stability of the device remain the internal factors which are rooted in the light-absorbing layer material and the contact between the light-absorbing layer and the charge-transport layers.[11] Specifically, the reasons for limiting stability are related to hygroscopicity, thermal degradation, and defects. Based on the aforementioned problems, the process engineering, composition engineering, and interface engineering are continuously optimized to reduce the defects or to increase resistance to humidity or temperature, with the ultimate goal to prepare stable PSCs.[12,13] As part of these ongoing efforts, materials such as 2D perovskites,[14] metallic oxides,[15] 2D materials,[16] polymers,[17] fullerene derivatives,[18] and salts[19] have been introduced into perovskite films or at the interface area to improve the stability of the devices. Very recently, Yang et al.[20] designed an ammonium salt, cyclohexylethylammonium iodide (CEAI), for interfacial engineering to effectively improve the stability of PCSs due to the enhancement in the surface hydrophobicity and passivation. However, most of these functional materials are toxic or difficult to be designed with hydrophobic structure and chemical interaction with the perovskite, which can improve

F. Wang, C. Ge, D. Duan, H. Lin, H. Hu
Hoffman Institute of Advanced Materials
Shenzhen Polytechnic
Shenzhen 518000, China
E-mail: hanlinhu@szpt.edu.cn

L. Li
Department of Sciences and Engineering
Sorbonne University Abu Dhabi
Abu Dhabi P.O. 38044, United Arab Emirates
E-mail: liang.li@sorbonne.ae

L. Li, P. Naumov
Smart Materials Lab
New York University Abu Dhabi
Abu Dhabi P.O. 129188, United Arab Emirates
E-mail: pance.naumov@nyu.edu

P. Naumov
Molecular Design Institute
Department of Chemistry
New York University
100 Washington Square East, New York 10003, USA

The ORCID identification number(s) for the author(s) of this article can be found under https://doi.org/10.1002/sstr.202200048.

DOI: 10.1002/sstr.202200048

the stability of the devices, resulting in complex preparation process.[21] Therefore, the efforts to find suitable materials for improvement of the stability of PSCs are continuing.

In recent years, ionic liquids (ILs), being green functional solvents, have been regarded as potential alternatives to some traditional additives and interface modifiers to fabricate stable PSCs. This choice rests with their wide liquid-state range, designability, high carrier mobility, and thermal and electrochemical stability.[22–25] Caprioglio and colleagues reported a poly(ionic liquid) (PIL) as multifunctional interlayer to improve the stability of a device and the PIL-treated device had PCE of 21% during 10 months in an inert atmosphere without significant efficiency decrease.[26] The reason for the improvement of stability lies within the synergistic effect of the hydrophobic surface and reduction of defects induced by the PIL treatment. Bai et al. proposed an effective strategy for introducing 1-butyl-3-methylimidazolium tetrafluoroborate ($BMIMBF_4$) IL into perovskite film to improve the thermal stability of PSCs by enhanced chemical interaction between the perovskite and the IL with suppressed degradation of the perovskite layer.[27] These works have proven that ILs can indeed effectively improve the stability of the devices through different mechanisms. However, there are few reviews containing systematic discussion of the development of ILs-assisted perovskite film growth as well as of the application of ILs to the stability of PSCs. To promote the development of PSCs with long-term lifetime, in this review, we mainly focus on summarizing and analyzing the different mechanisms for improving device stability based on ILs. Specifically, strategies for introduction of hydrophobic groups, defect reduction and formation of chemical interactions are proposed and discussed. The stability performance parameters of PSCs with different ILs are also summarized. Finally, we put forward ideas for commercialization by improving the stability of devices by ILs.

2. Mechanism of Instability and Degradation of PSCs

The structure of PSCs is usually composed of electrode materials, perovskite photoactive layer, and electron- and hole-transport layer materials. Each layer of material in the structure plays a significant role in the performance of the devices and the stability as an important index of performance. Especially under complex external conditions such as light, heat, and humidity, each layer of the device may become unstable and degrade to a varying extent.[28] According to the function of each layer of material in PSCs, the contributions of the layers to the stability are divided into the perovskite layer and the other layers which will be discussed separately.

2.1. Instability Problems Based on Perovskite Layers

Different preparation processes such as spin-coating, two-step sequential deposition, blade coating, and blowing have been employed to prepare perovskite film in PSCs.[29] However, despite of the continuous optimization of these preparation processes, the instability of the perovskite layer has not been overcome yet. The defects on the surface and grain boundaries of perovskite films are known to be central to the instability of the perovskite layer.[30] These features are sensitive to humidity, oxygen, and heat, resulting in irreversible degradation of the PSCs, as shown in **Figure 1**. Being the light-absorbing layer material, the stability of the perovskite layer directly affects the stability performance of the device. Humidity is a major factor that affects the device stability, especially for perovskite films. Taking the most common methylammonium (MA)-based perovskite film $CH_3NH_3PbI_3$ as an example, this material decomposes to CH_3NH_3I and PbI_2 in a humid environment under the action of water. The most apparent manifestation of

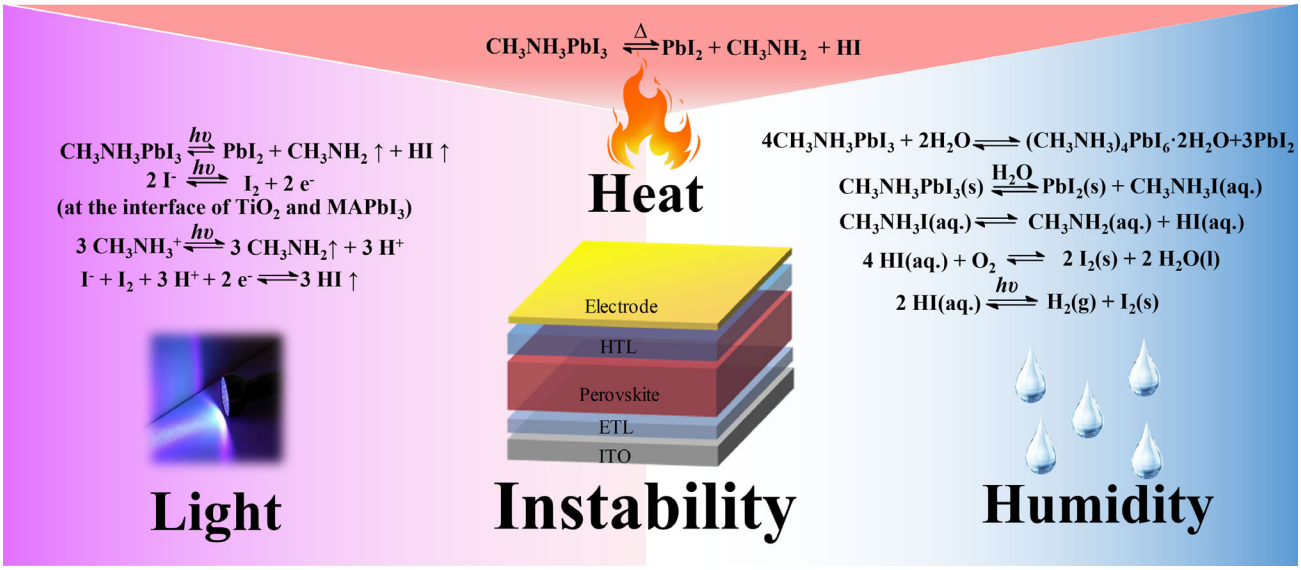

Figure 1. Schematic diagram of the instability of perovskite solar cells (PSCs) under the effect of different factors and chemical equations of the degradation processes under external factors such as humidity, heat, and light.

this process is gradual fading of the black perovskite films. In the initial stage of degradation, the intermediate products, a monohydrate $MAPbI_3{\cdot}H_2O$, and a dihydrate $(MA)_4PbI_6{\cdot}2H_2O$ were confirmed to appear successively.[31] When the perovskite films are continuously exposed to humid air, the strength of the hydrogen bond between the PbI_6 octahedral anion and the methylammonium cation is reduced by the water molecules and finally, an irreversible reaction occurs to form PbI_2.[32] In addition to the MA-based perovskite, a similar degradation phenomenon was discovered in FA-based perovskite under the effect of humidity. In 2014, Snaith and coworkers found that the FA-based perovskite exhibited the similar degradation rate to the MA-based perovskite when exposing the perovskites to a moist atmosphere.[33] Zhu and colleagues systematically investigated the degradation mechanism of $FAPbI_3$ in a dry desiccator with a constant humidity of 15% through the UV–Vis spectrum and the X-ray diffraction (XRD) pattern.[34] A significant absorption attenuation above 400 nm was found after humidity treatment over 18 days due to the perovskite decomposition and formation of PbI_2. After 30 days of storage in a desiccator, the signals of δ-$FAPbI_3$ and PbI_2 can be detected that further confirm the degradation of $FAPbI_3$ by humidity caused by the phase transition of α-$FAPbI_3$ to δ-$FAPbI_3$ and decomposition to PbI_2. Similarly, the purest $CsPbI_3$ films were sensitive to moisture, which limited the processing environment to nitrogen atmosphere.[35] The moisture accelerates the polymorphic transition of α-phase $CsPbI_3$ to δ-phase $CsPbI_3$ and leads to conversion from black perovskite to yellow non-perovskite.[36] The moisture–stability comparison between $CsPbI_3$ and $MAPbI_3$ was also investigated by Yin and the coworkers, and the relevant $CsPbI_3$-based PSCs can maintain 75% of the original PCE after 500 h under the average humidity of 45%–55%, which was obviously superior to 30% of the original PCE in $MAPbI_3$-based PSCs.[37]

Temperature plays a critical role in the stability of the perovskite films. A certain annealing temperature is required for the formation of high-quality films in the perovskite layer, and therefore the comprehensive understanding of the influence of temperature on the stability of perovskite is highly needed.[38,39] For MA-based perovskite materials, high temperature can cause decomposition of $MAPbI_3$ into HI, PbI_2, and CH_3NH_2, along with fading of the dark color of the initial perovskite films. The residual CH_3NH_2 in perovskite films can severely undermine the photoelectric properties of the device.[40] In contrast to $MAPbI_3$, $FAPbI_3$ exhibits slightly better thermal stability. However, $FAPbI_3$ also suffers from long-term stability problems. For example, the black phase of $FAPbI_3$ can be converted into a photo-inactive yellow δ phase below 150 °C.[2] Light-illumination is another important factor that affects the stability of the PSCs. Halogen free radicals would appear within a perovskite material under illumination with light and the perovskite material itself breaks down into halogen diatoms (I_2, Br_2, and Cl_2).[41] Meanwhile, light acts together with humidity, oxygen, and heat and can significantly accelerate the degradation of the PSCs.[42]

2.2. Instability Problems Based on Other Components

The stability of other layers such as electron-transporting layers (ETLs), hole-transporting layers (HTLs) and electrodes in the device directly affects the stability of the perovskite devices. TiO_2, ZnO, SnO_2, and C_{60} are widely applied as ETL materials to fabricate high-performance PSCs. Instability of TiO_2 was reported by Snaith et al.[43] under irradiation with UV light, and desorption of the surface-absorbed O_2 on mesoporous TiO_2 films is due to the sensitivity of the TiO_2 layer to UV light, leading to deep surface traps and instability of the device. ZnO was applied as a substitute for TiO_2 to improve the UV resistance of ETL in PSCs structure. Nevertheless, the instability still remains for ZnO-based PSCs. Yang et al.[44] discovered that acid–base chemical reaction and thermal decomposition of a perovskite film occur at the interface of the ZnO layer and the $CH_3NH_3PbI_3$ layer, and ultimately, the perovskite breaks up into methylamine and PbI_2 driven by this reaction. Similarly, the stability of PSCs is impacted by the instability of HTLs materials, such as is the case with the most common HTLs of 2,2′,7,7′-tetrakis(*N*,*N*-di-*p*-methoxyphenylamine)-9,9′-spirobifluorene (Spiro-OMeTAD) film. Qi and colleagues[45] discussed the decrease in performance in PSCs based on the instability of Spiro-OMeTAD layer with doping of Li-bis(trifluoromethanesulfonyl)-imide (LiTFSI). The presence of pinholes in the Spiro-OMeTAD layer resulted in formation of channels across the film, which facilitated the migration of LiTFSI from the bottom to the top and further affected the stability of perovskite layer. Poly(3,4-ethylenedioxythiophene)/poly(styrenesulfonate) (PEDOT:PSS) as another HTL material, whose negative impact on the stability of the device due to its hygroscopic properties, had been shown in previous work.[46] In addition, electrodes as charge collection layer in PSCs also suffer from instability. Metals such as Au, Ag, and Al were evaporated on the transport layer as the most common electrode materials of PSCs. However, as relatively cheap metal materials compared to Au, Ag and Al tend to react with the components in perovskite to form metal halides under humid conditions, which significantly diminishes the stability of the device. Specifically, the moisture first diffuses from the pinholes of the Spiro-OMeTAD to the perovskite layer, inducing the degradation of the perovskite film into HI, PbI_2, and CH_3NH_3I. These volatile iodine compounds migrate across the channel of Spiro-OMeTAD layer to react with Ag or Al electrode to form AgI (AlI_3). The continuous degradation of the perovskite and the generation of metallic compound further accelerate the damping of device stability.[47] Although Au is stable, it can still diffuse from the transport layer to the perovskite layer when heated, resulting in decrease of the overall performance of the device,[48] and the related high cost is not conducive to development to commercialization.

3. Strategies for Improving of the Stability of PSCs by ILs

Stability of the devices is regarded as an essential parameter to evaluate their performance, and as mentioned previously, there are urgent challenges with fabrication of stable devices that will respond to the requirements for practical applications. Diverse strategies such as additive engineering, preparation process engineering, interface engineering, and packaging engineering have been adopted to enhance the device performance and enable them to be more resilient to instability caused by both internal and external factors.[49] Among these engineering approaches, various kinds of functional materials have been considered for

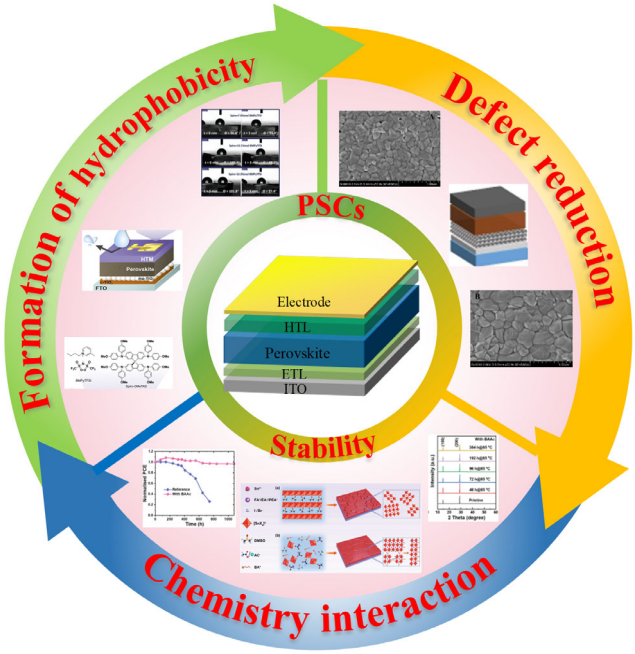

Figure 2. Illustration of strategies including enhanced hydrophobicity, defect reduction, and chemistry interaction for preparation of stable PSCs. Images for 'formation of hydrophobicity': Reproduced with permission.[63] Copyright 2018 Elsevier Inc. Images for 'defect reduction': Reproduced with permission.[66] Copyright 2019 Elsevier B.V. Images for 'chemistry interaction': Reproduced under the terms of the Creative Commons CC-BY license.[80] Copyright 2021, The Authors. Published by Wiley-VCH.

their potential in solving the problem of stability of the PSCs.[50] ILs have attracted special attention as such materials because of their nontoxicity and designability.[51–53] In this section, we mainly summarize and focus on strategies for improving the stability of PSCs by ILs (**Figure 2**).

3.1. Enhancement of Hydrophobicity

The sensitivity of the PSCs to humidity can be controlled by formation or introduction of hydrophobic groups, which have been demonstrated to effectively inhibit the decomposition of the device in humid environment.[26,54] Taking the advantages of chemical variations, ILs are easy to provide PSCs with hydrophobic groups and to enhance the resistance to water molecules in humid environment.[55–57] **Table 1** summarizes the photovoltaic parameters of stable ILs-treated PSCs through hydrophobicity. Liu et al.[58] added fluorinated IL additive, methylammonium trifluoroacetate ($MA^+CF_3COO^-$, MA^+TFA^-) into the perovskite precursor solution to significantly enhance the ambient stability of PSCs (**Figure 3**a). A small amount of MA^+TFA^- is distributed in the grain boundaries after the annealing of the perovskite film, which turns the grain boundaries hydrophobic on account of the multiple fluorocarbon groups in MA^+TFA^-. Furthermore, the hydrophobicity of MA^+TFA^- improved the wettability and reduced heterogeneous nucleation, leading to the formation of perovskite films with large grain domains. As a result, the PSCs based on MA^+TFA^--treated perovskite film exhibited efficiency decay of only 11% after 336 h at 40% relative humidity (RH). Similarly, multiple fluorocarbon groups in 1-methyl-3-(1*H*,1*H*,2*H*,2*H*-nonafluorohexyl) imidazolium iodide (FIm) were confirmed by Salado et al.[57] to have a stabilizing effect on the PSCs (Figure 3b). From the results of XRD measurements, inconspicuous decomposition occurred in 1% FIm-treated $Cs_{0.05}(MA_{0.15}FA_{0.85})_{0.95}Pb(I_{0.85}Br_{0.15})_3$ perovskite film after 33 days in RH environment of 55–60% and well-defined signal of PbI_2 appeared in $Cs_{0.05}(MA_{0.15}FA_{0.85})_{0.95}Pb(I_{0.85}Br_{0.15})_3$ perovskite film, which indicated the inhibitory effect on decomposition reaction of the IL FIm. The corresponding 1% FIm-treated PSCs remained even more stable for over 1 month in 50–55% RH. Based on the same mechanism, application of the IL 1,3-*bis*(cyanomethyl)imidazolium *bis*(trifluoromethylsulfonyl)imide ([Bcim][TFSI]) containing multiple fluorocarbon groups to increase the device lifetime had been reported by Gao et al.[23]

Moreover, ILs containing long alkyl chains based on imidazole groups have also been developed as additives to enhance the stability of perovskite films. Akin et al.[59] employed 1-hexyl-3-methylimidazolium iodide (HMII) IL as an additive in $FAPbI_3$-based PSCs to suppress the transition from the black phase (α-$FAPbI_3$) to the non-perovskite yellow phase (δ-$FAPbI_3$) for stabilization of the PSCs (Figure 3c,d). The grain coarsening and defects

Table 1. Summary of the photovoltaic parameters of stable ILs-treated PSCs via hydrophobicity.

ILs	Device structure	PCE [%]	Stability	References
MA^+TFA^-	FTO/TiO_2/$MAPbI_3$/Spiro-OMeTAD/Au	20.10	336 h, 40% RH, room temperature (RT), 80% of PCE	[58]
FIm	FTO/TiO_2/$Cs_{0.05}(MA_{0.15}FA_{0.85})_{0.95}Pb(I_{0.85}Br_{0.15})_3$ Spiro-OMeTAD/Au	16.32	150 days 55–60% RH, Stable	[57]
[Bcim][TFSI]	FTO/cp-TiO_2/mp-TiO_2/SnO_2/$(Cs_{0.08}FA_{0.8}MA_{0.12})Pb(I_{0.88}Br_{0.12})_3$ /PEAI/HTM/Au	21.06	150 days 20–30% RH exceed 90% of PCE	[23]
HMII	FTO/c-TiO_2/mp-TiO_2/$FAPbI_3$/Spiro-OMeTAD/Au	20.60	250 h, 60% ± 10% RH, 80% of PCE	[59]
HMImCl	FTO/TiO_2/$MAPbI_3$/NPs/CsFAMA/Spiro-OMeTAD/Au	19.44	6000 h, 30−40% RH, 90% of PCE	[60]
$DMIMPF_6$	FTO/TiO_2/$Cs_{0.08}FA_{0.92}PbI_3$/$DMIMPF_6$/spiro-OMeTAD/Au	23.25	3 h, continuous illumination, 90% of PCE 480 h, 45% RH, 89% of PCE	[62]
BMPyTFSI	FTO/c-TiO_2/mp-TiO_2/$Cs_{0.1}(FAPbI_3)_{0.81}(MAPbBr_3)_{0.09}$/ FDT/Au	18.24	NA	[64]
BMPyTFSI	FTO/c-TiO_2/mp-TiO_2/$(FAPbI_3)_{0.85}(MAPbBr_3)_{0.1}$/Spiro-OMeTApD/Au	14.96	200 days, 50% RH, 80% of PCE	[63]
$APMimPF_6$	ITO/TiO_2/$C_7H_{16}N_3PbI_3PF_6$/ CuSeCN/Au	17.30	2 months, 57% RH, 98% of PCE	[56]
[BMMIm]Cl	FTO/c-TiO2/*m*-TiO_2/$CsPbBr_3$/[BMMIm]Cl/carbon	9.92	30 days, 70% RH, 99.3% of PCE	[83]
[bvbim]Cl)	FTO/TiO_2/$MAPbI_3$/Spiro-OMeTAD/Au	19.92	1000 h, 45 ± 5% RH, 90% of PCE	[54]

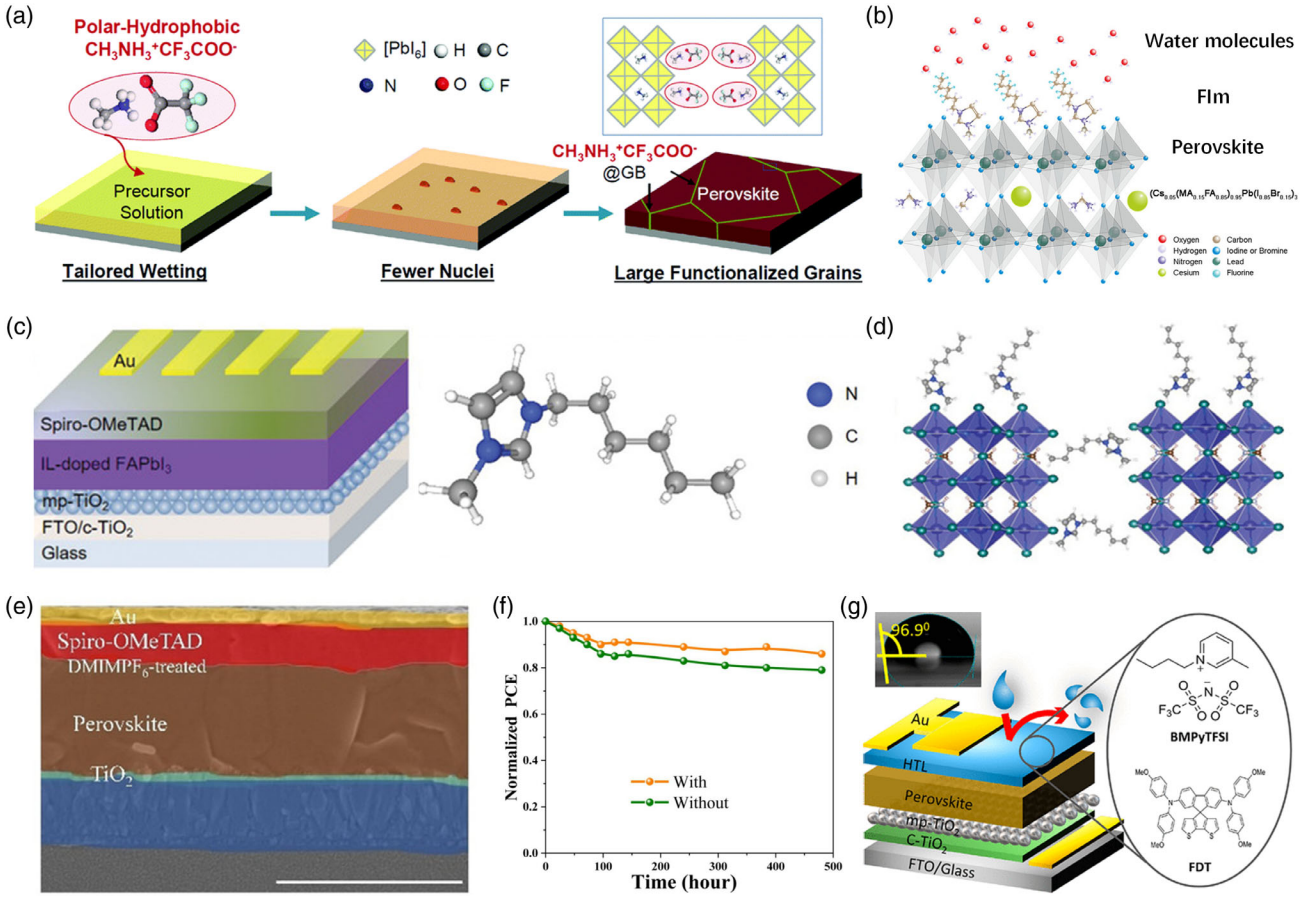

Figure 3. a) Schematic diagram of hydrophobic ionic liquids (IL) $MA^+CF_3COO^-$-assisted crystallization of $MAPbI_3$ perovskite thin films. Reproduced with permission.[58] Copyright 2019, The Royal Society of Chemistry. b) Schematic diagram of the role and interaction of fluorocarbon groups in 1-methyl-3-(1*H*,1*H*,2*H*,2*H*-nonafluorohexyl) imidazolium iodide (FIm) on perovskite layer. Reproduced with permission.[57] Copyright 2017, Wiley-VCH. c) Schematic illustration of devices structure and molecular structure of the 1-hexyl-3-methylimidazolium (HMI^+). d) Schematic diagram of effects of HMI iodide (HMII) IL on perovskite $FAPbI_3$ active layer. Reproduced with permission.[59] Copyright 2020, Wiley-VCH. e) Cross-sectional scanning electron microscope (SEM) images of $DMIMPF_6$-treated perovskite device. f) Normalized power conversion efficiencies (PCEs) of perovskite devices stored at 45% relative humidity for 480 h. Reproduced with permission.[62] Copyright 2020, Wiley-VCH. g) Schematic diagram of the IL BMPyTFSI-treated PSCs based on the (2′,7′-bis(bis(4-methoxyphenyl)amino)spiro-[cyclopenta[2,1-b:3,4-b′]dithiophene-4,9′-fluorene]) (FDT) as hole-transporting layers (HTL). Reproduced with permission.[64] Copyright 2020, American Chemical Society.

reduction induced by HMII IL promote the enhancement of PCE to 20.6%. In terms of device stability, the pristine film experienced obvious transition process of the black phase to the yellow phase and the absence of non-perovskite δ-phase was observed in HMII-assisted perovskite films after 10 days in RH of about $60 \pm 10\%$ from the XRD patterns, indicative of considerably enhanced resistance to moisture due to the high hydrophobicity of the long alkyl chain in HMII IL. The chemical interaction between the perovskite material and IL HMII molecules has strongly suppressed the migration of ions, which effectively inhibits the phase transition from the black phase to the yellow phase, stabilizing the existence of the black phase of the perovskite material. The control PSCs only remain 70% of the original PCE after 30 h at $60\% \pm 10\%$ RH without encapsulation, whereas the HMII-treated PSCs maintained over 80% of original PCE after 250 h under the same conditions. Shahiduzzaman et al.[60,61] reported that 1-hexyl-3-methylimidazolium chloride (HMICl)-assisted perovskite can significantly improve the stability of the perovskite device due to the hydrophobicity of its long alkyl chain.

By addition of IL as additives into the perovskite precursor solution to provide hydrophobic groups, researches have reported that ILs can be employed in the interfaces of PSCs via interfacial engineering to improve the humidity stability based on the introduction of hydrophobic groups. Zhu et al.[62] introduced 1,3-dimethyl-3-imidazolium hexafluorophosphate ($DMIMPF_6$) IL into the interface between the perovskite layer and the electron transport layer to enhance the stability of the PSCs due to the hydrophobic group of $DMIMPF_6$ (Figure 3e). The hydrophobic properties of the $DMIMPF_6$ layer suppressed moisture permeation efficiently, resulting in significantly enhanced stability in a high-humidity environment. Unencapsulated $DMIMPF_6$-treated devices retained 89% of their initial PCE after 480 h in 45% relative humidity, which was significantly superior to stability of a control device with 20% loss in the PCE under the same conditions (Figure 3f). Moreover, the

heat stability of the $DMIMPF_6$-treated device was also confirmed to be improved compared to the control device. The $DMIMPF_6$ device maintained 90% of its initial efficiency after 3 h at 65 °C while the control device showed a significant decline in efficiency.

Spiro-OMeTAD with LiTFSI was often used in the HTL layer of the PSCs structure. However, the moisture was absorbed from the atmosphere by the lithium salts due to their strong hygroscopicity, leading to degradation of HTL under high humidity in the atmosphere. Based on the instability of the transport layer, ILs were adopted in the transport layer engineering to improve the stability of PSCs. Calio et al.[63]proposed a new strategy for enhancing the longevity of devices through the hydrophobic 1-butyl-3-methylpyridinium bis(trifluoromethylsulfonyl)imide (BMPyTFSI) IL-based doping in HTL layer. According to optical images recorded by optical microscope and scanning electron microscope (SEM), the HTL film with BMPyTFSI as dopant showed the characteristics of uniformity and smoothness with fewer pinholes. Meanwhile, the contact of the interface between the HTL and the perovskite layer was also significantly improved. These consequences pointed toward the effects of IL BMPyTFSI in promoting the formation of high-quality HTL film. The contact-angle value of Spiro-OMeTAD with IL BMPyTFSI was further illustrated with a significant increase from a lower value of 78° of conventional doped layer to 90° due to the introduction of hydrophobic groups, which cooperated with reduced pinholes to prevent the diffusion of moisture. BMPyTFSI-treated Spiro-OMeTAD-based PSCs showed only 20% loss of efficiency over 7 months in humid (50% RH) conditions and the contrast was obvious with conventional doped PSCs, which showed a 50% decrease compared to its initial efficiency. Similarly, Ahmad et al.[64] reported that IL BMPyTFSI was introduced into the HTL material of FDT (2′,7′-bis(bis(4-methoxyphenyl)amino) spiro-[cyclopenta[2,1-b:3,4-b′]dithiophene-4,9′-fluorene]) to control the water sensitive of PSCs through hydrophobicity of IL BMPyTFSI (Figure 3g). The contact angle (with deionized [DI] water) of pristine FDT-based HTM was <80°, while for the FDT-based HTM with 16 mol% of BMPyTFSI-doped one it has remarkably increased to 97°, which explained the function of IL BMPyTFSI on protecting perovskite layer from moisture absorption for long-term stability of PSCs. These strategies of hydrophobic IL doping on the HTL could boost the conductivity and hole mobility, which was beneficial to optimize the efficiency of the device. In contrast, they extended the operational lifetime of the device and ensured durability of the device.

3.2. Defect Reduction

Previous studies had reported that defects at grain boundaries and interfaces are particularly important in causing device instability.[65] These areas are prone to irreversible degradation of the PSCs owing to their sensitivity to factors such as oxygen, moisture, and heat. Therefore, searching for appropriate strategies to reduce these defects could effectively improve the resistance to instability of the PSCs under the aforementioned factors. ILs have been widely confirmed to promote formation of high-quality perovskite films with fewer defects and to reduce interface defects. The photovoltaic parameters of stable ILs-treated PSCs through defect reduction are summarized in **Table 2**.

Zhou et al.[66] reported that by mixing 1-ethylamine hydrobromide-3-methylimidazolium hexafluorophosphate ($ILPF_6$) with the perovskite precursor solution, it is possible to obtain high-efficiency and stable carbon-based hole-conductor-free PSCs based on $ILPF_6$-treated perovskite film with large grain size and low concentration of defects (**Figure 4**a). From the results obtained by SEM, the control perovskite film possessed poor crystal quality with many grain boundaries and the improvement was obvious with enhancement of crystalline quality in $ILPF_6$-treated perovskite film, which was attributed to the effect of $ILPF_6$ on optimization of the crystallization and morphology by suppressing the nucleation and decreasing the crystallization growth rate (Figure 4b). Ultimately, unencapsulated $ILPF_6$-treated PSCs could retain 94% of their initial PCE in RH of 20% after 840 h due to reduction of defects at grain boundaries for blocking the infiltration of water, which was significantly better than the 52% with the control device. This strategy of introducing ILs to reduce defects for improving device stability is more remarkable in $FASnI_3$ PSCs. Poor crystallinity and quality of the film usually occur in $FASnI_3$ PSCs because of the faster reaction of FAI and SnI_2 than FAI and PbI_2 in the crystallization process, leading to the existence of redundant defects at the grain boundary and the surface of the films.[67] Recently, the IL formamidine acetate (FAAc) as an additive was introduced into perovskite precursor solution by Xu et al.[68] to regulate the crystallization of the perovskite for preparation of high-quality

Table 2. Summary of the photovoltaic parameters of stable ILs-treated PSCs through defect reduction.

ILs	Device structure	PCE [%]	Stability	References
ImI	FTO/c-TiO_2/*m*-TiO_2/ $MAPbI_3$/ImI/Spiro-OMeTAD/Au	19.90	300 h, light (100 mW cm^{-2}) NA	[65]
$ILPF_6$	FTO/c-TiO_2/*m*-TiO_2/$MAPbI_3$/carbon	13.01	840 h, 20% RH, 25 °C, 94% of PCE	[66]
FAAc	ITO/PEDOT:PSS/$FASnI_3$/C_{60}/BCP/Ag	9.96	1600 h, light, N_2, 82% of PCE	[68]
BMIBr	ITO/PEDOT:PSS/PVK-BMIBr)/PCBM/BCP/Ag	10.09	1200 h, N_2, 85% of PCE 48 h, 50% RH, 40% of PCE	[70]
$FB^+BF_4^-$	ITO/SnO_2/$(FAPbI_3)_{1-x}(MAPbBr_3)_x$/Spiro-OMeTAD/Au	22.52	2000 h, 30%, 25 °C, 80% of PCE 2000 s, Sun illumination, 96% of PCE	[69]
$BMIMBF_4$	FTO/NiO_x/$CsPbI_2Br$/$BMIMBF_4$/$PC_{61}BM$/BCP/Ag	13.21	1080 h, N_2, 86.9% of PCE 500 h, 35% RH, 82% of PCE	[72]
$BMIMPF_6$	FTO/TiO_2/$BMIMBF_6$/$CsPbI_2Br$/carbon	13.19	60 days, 20% RH, 91% of PCE	[73]

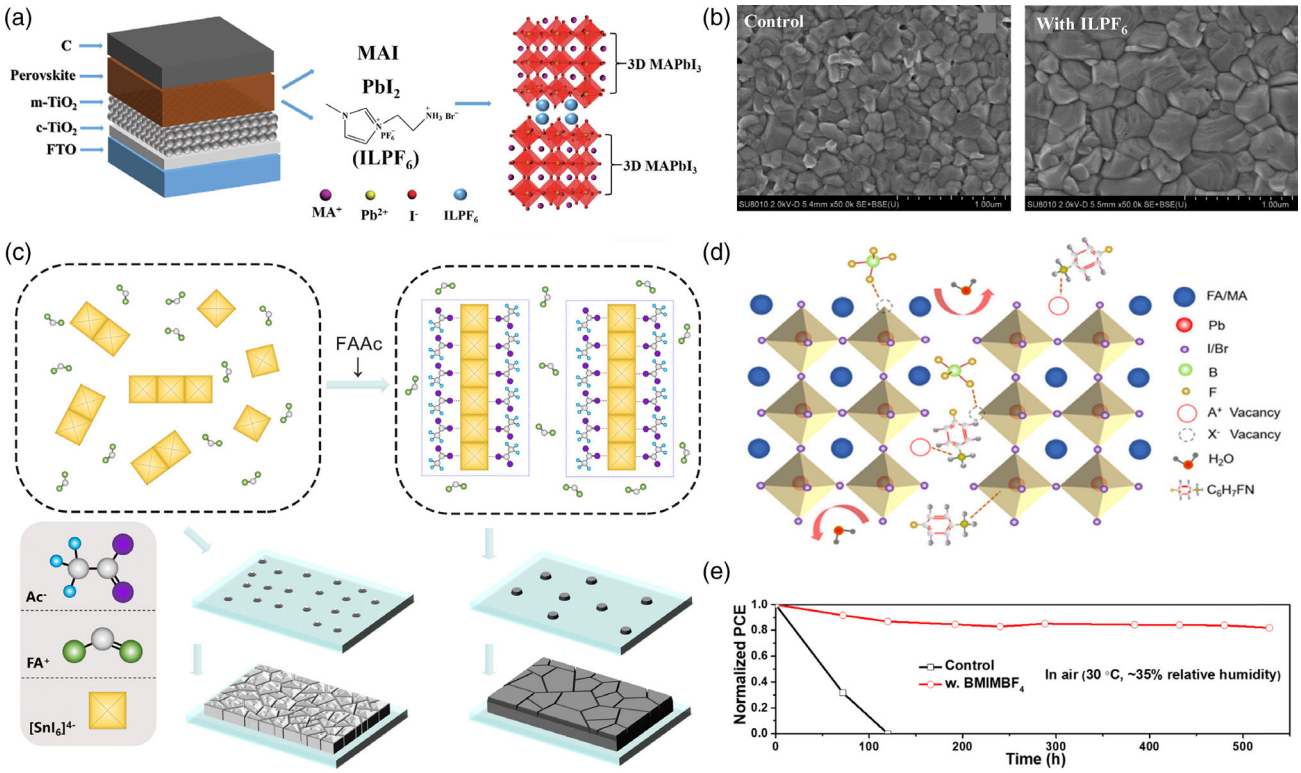

Figure 4. a) Structure diagram for the glass/fluorine doped tin Oxide (FTO)/c-TiO_2/*m*-TiO_2/$ILPF_6$-perovskite/carbon–based PSCs. b) SEM images of the control and $ILPF_6$-treated $CH_3NH_3PbI_3$ perovskite films. Reproduced with permission.[66] Copyright 2019, Elsevier B.V. c) Schematic diagram of IL formamidine acetate (FAAc)-assisted perovskite crystallization process. Reproduced with permission.[68] Copyright 2021, American Chemical Society. d) Schematic diagram of defect passivation by IL for the improvement of solar cell performance and stability. Reproduced with permission.[69] Copyright 2021, Wiley-VCH. e) Stability test in air (30 °C, 35% relative humidity) of control and 1-butyl-3-methylimidazolium tetrafluoroborate ($BMIMBF_4$)-treated devices. Reproduced with permission.[72] Copyright 2020, Elsevier Ltd.

$FASnI_3$ film (Figure 4c). Taking advantage of the inhibiting effect on the oxidation process of Sn^{2+} to Sn^{4+} by slower crystal growth, FAAc played an important role in obtaining high-quality films and effectively reduced defects. Hence, the IL FAAc-treated device retained 82% of its initial PCE after 1600 h, while the control device displayed an arresting damping in PCE within <200 h. The additive zwitterionic IL (ZIL) with tetrafluoroborate (BF_4^-) as anions and phenylammonium ($4FB^+$) as cations has also been employed in two-step deposition method for defect passivation to obtain a high-quality perovskite thin film, leading to enhanced stability.[69] Specifically, the organic anionic and cationic defects in a perovskite were effectively passivated by anchoring of the uncoordinated Pb^{2+} by the $4FB^+$ cation and reduction of halogen defects by the BF_4^- anion (Figure 4d). Moreover, 1-butyl-3-methylimidazolium bromide (BMIBr)[70] and 1-ethyl-3-methylimidazolium hydrogen sulfate ($EMIMHSO_4$)[71] ILs as additives in the perovskite precursor solution have also been confirmed to reduce the defects for long-life PSCs. Except for the effect of the above ILs as additives in the precursor solution, the ILs can also be employed as interface modifiers to decrease the defects on the perovskite surface and to optimize the contact of the interface. Wang et al.[72] developed a new strategy to stabilize the $CsPbI_2Br$ phase and to reduce the surface defect density through placement of $BMIMBF_4$ as interface modifiers between the perovskite layer and the PCBM layer. After $BMIMBF_4$ modification of the interface, they observed uniform thickness, excellent adhesion to the NiO_x substrate and higher film quality with significantly reduced pinholes. As a consequence, the corresponding $BMIMBF_4$-treated PSCs acquired stability by retaining 86.9% of the original PCE over 1000 h in N_2 atmosphere and 82% of the original PCE after 500 h in 35% RH (Figure 4e). Similarly, BMIM-based IL 1-butyl-3-methylimidazole hexafluorophosphate ($BMIMPF_6$) was used as interface modification layer that is located on the interface of the perovskite layer and the TiO_2 layer for improvement of the device stability by Yin et al.[73] The interface modification of the IL $BMIMPF_6$ played an important role in the passivation of perovskite film defects and optimization of the contact of the TiO_2/$CsPbI_2Br$ interface.

3.3. Chemistry Interaction

In addition to strategies of introducing hydrophobic groups and reducing defects by ILs for improving the stability of the device, chemical interaction was often considered between the ILs and the perovskite component due to the designability of ILs, which also affected the stability of the device.[22,74–76] The specifically designed ILs contained the COO^- or HSO_4^- groups that possess the ability to coordinate with Pb^{2+} or Sn^{2+}, which can contribute

to the formation of high-quality film for improvement of stability.[71,77] Moreover, the functionalized ILs with imidazolium group or quaternary ammonium groups, which are enabled with the ability to form hydrogen bonds with the I^-, Br^-, and Cl^- in perovskite materials, effective anchoring the I^-, Br^-, and Cl^- for inhibition of instability caused by ion migration.[78] The formation of O···H–N hydrogen bonds between the carboxyl and ester groups in ILs with MA^+ or FA^+ also leads to the stabilization of organic ions.[79]

The photovoltaic parameters of stable ILs-treated PSCs through chemical interaction are summarized in **Table 3**. Li et al.[80] employed the IL *n*-butylammonium acetate (BAAc) to regulate crystallization of the perovskite crystals through the O···Sn chelating bonds between $Ac^-(CH_3COO^-)$ and Sn(II) and the N–H···X hydrogen bonds by interaction between BA^+ and X-site anions (**Figure 5**a). Taking advantage of the multiple bonds between BAAc and SnI2, the retarded crystal growth rate of the perovskite films led to the formation of high-quality films with less defect states. Furthermore, the existence of the hydrogen bonds (NH···I) in the ammonium group of BA^+ and I^- effectively suppresses the migration of I^- to the surface of the perovskite film, reducing the defects caused by I^-. Moreover, the formation of the strong coordination between Ac and Sn(II) through the incorporation of IL BAAc can remarkably inhibit the oxidation of Sn(II) to Sn(IV), maintaining the stability of Sn(II) (Figure 5b). Based on the positive role of IL BAAc, the BAAc-treated PSCs provided significantly improved PCE of 10.4%, which was obviously better than that of the control device at 8.6%. More importantly, the corresponding PSCs showed excellent thermal stability and preserved 80% efficiency of the initial value after 400 h at 85 °C. Instability also exists in MA-based perovskite devices, as a result of the migration of MA^+ from the bulk to the crystal surface followed by the formation of MA by the fleeing MA^+ from the crystal lattice under external effects. Recently, Wang et al.[81] reported an effective strategy for anchoring the MA^+ via hydrogen bonding and enhancement of the Pb–O interaction by methylammonium difluoroacetate (MA^+DFA^-) (Figure 5c). In view of the interaction between fluorinated anion CF_2HCOO^- in IL MA^+DFA^- and MA^+ in perovskite precursor solution, the stability of the perovskite crystal structure at surfaces and at the grain boundaries was improved. Ultimately, the stability of the devices under atmospheric and thermal conditions showed obvious improvement with 85% of the initial PCE after 180 days. The same anchoring effect via bonding between IL BMIBr and the perovskite film had been proved to play a role in the thermal stability by Du et al.[82]

Another IL, $BMIMBF_4$, had also been verified to play a significant role in stability by Bai et al.[27] The anion and cation in ILs showed different distributions in perovskite films based on the results from the time-of-flight secondary-ion mass spectrometry (ToF-SIMS) and while the cation $BMIM^+$ dispersed throughout the perovskite film, the anion BF_4^- mainly existed at the interface. On the basis of the distribution of the anion and the cation in the perovskite film and the stability experiment by replacing anion BF_4^- or cation $BMIM^+$, respectively, the improved stability was attributed to the accumulated BMIM cations, which bind to surface sites by chemical interaction to increase resistance to degradation of the perovskite layer. Wang et al.[79] produced an IL poly(1-vinyl-3-ethyl-acetate) imidazole tetrafluoroborate (PEa poly-RTMS) to improve the stability and efficiency of PSCs. The existence of PEa poly-RTMS not only passivated Pb^{2+} defects in the perovskite film through the abundant C=O groups with strong bonding affinity, but also added to the perovskite film hydrophobicity and strong resistance under high temperature and continuous light illumination (Figure 5d, e). In contract to the ILs RTMS, PEa poly-RTMS formed by polymerization of ILs contains the repeating units with the C=O groups passivating the Pb^{2+} defects and multiple anchor points through the chemical interaction possess strong bonding stability. Moreover, PEa poly-RTMS with the high decomposition temperature of 347 °C compared to IL RTMS and higher hydrophobicity from the polymer chain skeleton enhance the device stability. As a result, the PEa poly-RTMS-treated PSCs displayed a high PCE of 21.4% and a long-term operational stability that remained more than 92% of its initial efficiency after 1200 h at 70−75 °C. Taking the advantage of formation of chemical interaction in the multiple repeating units, the PILs [poly-1,3-*bis*(4-ethylbenzyl)-imidazolium chloride (PIL-[bebim]Cl)],[54] [poly-1-vinyl benzyl-triethylammonium chloride (PIL-Am)], and

Table 3. Summary of the photovoltaic parameters of stable ILs-treated PSCs through chemistry interaction.

ILs	Device structure	PCE [%]	Stability	References
RATZ	ITO/TiO_2/MA/RATZ)/spiro-OMeTAD/Au	20.03	3500 h, 40 ± 5% RH, 80% of PCE 50 h, 80 ± 5% RH, 80% of PCE	[22]
MPIB	ITO/PEDOT:PSS/MPIB-perovskite/$PC_{61}BM$/BCP/Ag	18.22	150 h, 40–60%, RT, 78% of PCE 30 min, 85 °C, 97% of PCE	[74]
IL with CC_2	FTO/c-TiO_2/meso-TiO_2/$MAPbI_3$/spiro-OMeTAD/Au	19.21	460 h, Ar, constant illumination of 100 mW cm^{-2}, 55% of PCE	[75]
$EMImBF_4$	FTO/NiO/PVK/$EMImBF_4$/PCBM/BCP/Ag	19.00	30 days, 25 °C, 20% RH, 90% of PCE	[76]
BAAc	FTO/PEDOT:PSS/$FASnI_3$/C_{60}/BCP/Ag	10.40	1000 h, N_2, 96% of PCE 400 h, 85 °C, 80% of PCE	[80]
MA^+DFA^-	(ITO)/CPTA/$(FA)_{0.15}(MA)_{0.85}PbI_{2.55}Br_{0.45}$/Spiro-OMeTAD/$MoO_x$/Ag	21.46	180 days, N_2, RT, 85% of PCE 120 h, 85 °C, 87.9% of PCE	[81]
BMIBr	FTO/TiO_2/$MAPbI_3$/spiro-OMeTAD/Au	10.55	20 min, 85 °C, 85% of PCE	[82]
$BMIMBF_4$	FTO/NiO/$(FA_{0.83}MA_{0.17})_{0.95}Cs_{0.05}Pb(I_{0.9}Br_{0.1})_3$/spiro-OMeTAD/Au	19.80	100 h, 60–65 °C, 86% of PCE	[27]
poly-RTMS	ITO/NiOx/poly-RTMS-FAMACs/PCBM/BCP/Cr/Au	21.47	5000 h, RT, 35 ± 5% RH, 94% of PCE 1200 h, 70–75 °C, 40 ± 5% RH, 92% of PCE	[79]

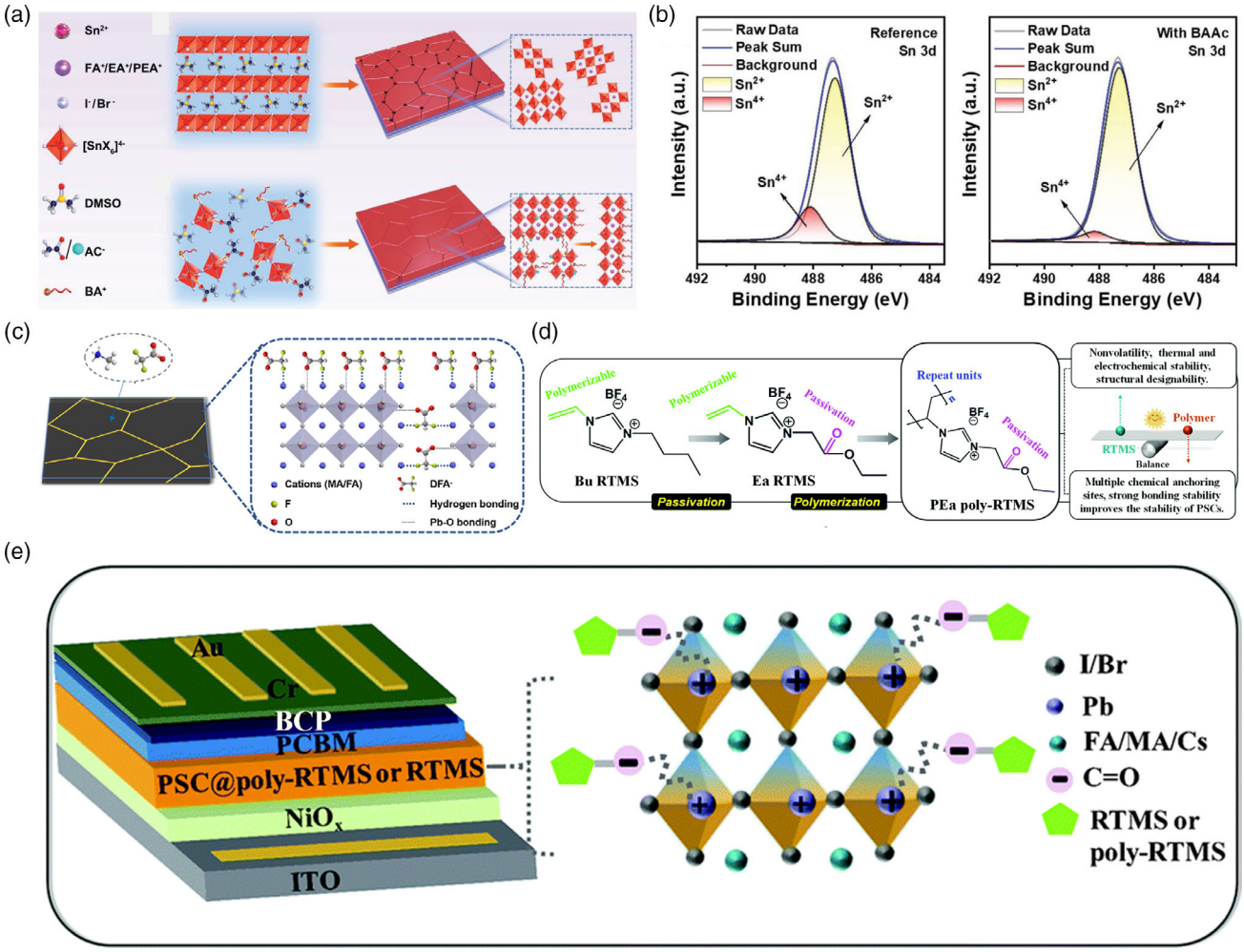

Figure 5. a) Schematic diagram of IL *n*-butylammonium acetate (BAAc)-assisted crystallization kinetics of Sn-based perovskite films. b) High-resolution X-ray photoelectron spectroscopy (XPS) spectra of Sn 3d for reference film and IL BAAc-treated films. Reproduced under the terms of the Creative Commons CC-BY license.[80] Copyright 2021, The Authors. Published by Wiley-VCH. c) Schematic diagram of the interactions between MA^+DFA^- and perovskites. Reproduced with permission.[81] Copyright 2020, Wiley-VCH. d) Chemical structure analysis and design of IL and poly(ionic liquid) (PIL). e) Schematic diagram of the interactions between PIL and perovskites. Reproduced with permission.[79] Copyright 2020, The Royal Society of Chemistry.

[poly-1-vinyl benzyl-3-methylimidazole chloride (PIL-Im)][78] have been also employed to improve device stability. These PILs that combine the advantage of polymers and ILs include the structural designability, excellent chemical durability and thermal stability, which adds to the polymerizable ILs or PILs the potential of prolonging the service life of the device.

4. Summary and Prospects

The unfavorable stability of the PSCs stands as an important problem to be overcome en route to commercialization of PSCs. As one of the strategies to overcome this challenge, ILs as functional materials are introduced into PSCs and effectively improve the stability of the devices. In this review, we focus on the analysis of the reasons for the instability of each individual part of the device and the degradation of the device based on both external and intrinsic factors. For the perovskite layer, we mainly concentrate on the discussion of the decomposition mechanism and processes of MA-based, FA-based, and all-inorganic-based perovskite films under different factors. Moreover, a deep understanding on the device degradation caused by the instability of transport layer materials and electrode materials is summarized. According to the causes of these instabilities, we also summarize the strategies for improving the stability of the devices by ILs, including the effects of increased hydrophobicity, defect reduction, and chemistry interaction. Specifically, we note that hydrophobic groups with the fluorocarbon groups, polymer chain, and long alkyl chains based on imidazole groups are introduced by chemically specially designed ILs, which effectively enhances the resistance of perovskite devices to humidity to inhibit the penetration of water in the PSCs. Another strategy is defect reduction by adding ILs into devices, which can control the sensitivity of the device to the external environment and contribute to the delayed

degradation of the device. The designed ILs generally are employed through additive engineering and interface modification engineering for grain boundaries and interfaces defects. Moreover, introducing chemical interaction between the ILs and the perovskite is an effective strategy to improving the stability of the devices. Even though several remarkable achievements of applications have been reported, the mechanism of the improved stability of PSCs with ILs remains unclear. Therefore, we summarize the challenges and prospects as follows. The design and selection of ILs need to be further explored, and the effect on stability of PSCs based on the structure of ILs needs to be explicated. An in-depth understanding of the specific chemical interaction between the designed ILs and the perovskite for anchoring the organic and inorganic ions in perovskite can effectively promote the device stability. Therefore, selecting the appropriate ILs based on their structure for perovskite devices is promising to extend the operational lifetime of the devices. The intermediate phase produced by the interaction between the ILs and the perovskite requires further consideration, which will generate the complex effects on crystallization and stability of the perovskite films. Furthermore, the mechanism of the influence of different anions and cations in the ILs on the temporary phase needs to be researched. At present, most of the preparation processes of high-stability PSCs based on ILs are spin coating, while blade-coating and large-scale roll-to-roll technologies are rarely explored.

After addressing these issues, we believe that the ILs hold a great potential for obtaining highly efficient, stable PSCs.

Acknowledgements

The financial support from the National Natural Science Foundation of China (Grant nos. 62004129 and 22005202) is gratefully acknowledged. The authors thank New York University, Abu Dhabi and Sorbonne University Abu Dhabi for financial supports.

Conflict of Interest

The authors declare no conflict of interest.

Keywords

crystal growth, ionic liquids, perovskites, photovoltaics

Received: March 16, 2022
Revised: April 25, 2022
Published online:

[1] H. Min, D. Y. Lee, J. Kim, G. Kim, K. S. Lee, J. Kim, M. J. Paik, Y. K. Kim, K. S. Kim, M. G. Kim, T. J. Shin, S. Il Seok, *Nature* **2021**, *598*, 444.

[2] J. Jeong, M. Kim, J. Seo, H. Lu, P. Ahlawat, A. Mishra, Y. Yang, M. A. Hope, F. T. Eickemeyer, M. Kim, Y. J. Yoon, I. W. Choi, B. P. Darwich, S. J. Choi, Y. Jo, J. H. Lee, B. Walker, S. M. Zakeeruddin, L. Emsley, U. Rothlisberger, A. Hagfeldt, D. S. Kim, M. Grätzel, J. Y. Kim, *Nature* **2021**, *592*, 381.

[3] M. Jeong, I. W. Choi, E. M. Go, Y. Cho, M. Kim, B. Lee, S. Jeong, Y. Jo, H. W. Choi, J. Lee, J. H. Bae, S. K. Kwak, D. S. Kim, C. Yang, *Science* **2020**, *369*, 1615.

[4] H. Hu, M. Qin, P. W. K. Fong, Z. Ren, X. Wan, M. Singh, C. J. Su, U. S. Jeng, L. Li, J. Zhu, M. Yuan, X. Lu, C. W. Chu, G. Li, *Adv. Mater.* **2021**, *33*, 2006238.

[5] H. Zhang, M. Qin, Z. Chen, W. Yu, Z. Ren, K. Liu, J. Huang, Y. Zhang, Q. Liang, H. T. Chandran, P. W. K. Fong, Z. Zheng, X. Lu, G. Li, *Adv. Mater.* **2021**, *33*, 2100009.

[6] J. Y. Kim, J. W. Lee, H. S. Jung, H. Shin, N. G. Park, *Chem. Rev.* **2020**, *120*, 7867.

[7] N. Li, X. Niu, L. Li, H. Wang, Z. Huang, Y. Zhang, Y. Chen, X. Zhang, C. Zhu, H. Zai, Y. Bai, S. Ma, H. Liu, X. Liu, Z. Guo, G. Liu, R. Fan, H. Chen, J. Wang, Y. Lun, X. Wang, J. Hong, H. Xie, D. S. Jakob, X. G. Xu, Q. Chen, H. Zhou, *Science* **2021**, *373*, 561.

[8] L. Meng, J. You, Y. Yang, *Nat. Commun.* **2018**, *9*, 5265.

[9] W. Hui, L. Chao, H. Lu, F. Xia, Q. Wei, Z. Su, T. Niu, L. Tao, B. Du, D. Li, Y. Wang, H. Dong, S. Zuo, B. Li, W. Shi, X. Ran, P. Li, H. Zhang, Z. Wu, C. Ran, L. Song, G. Xing, X. Gao, J. Zhang, Y. Xia, Y. Chen, W. Huang, *Science* **2021**, *371*, 1359.

[10] J. Li, R. Xia, W. Qi, X. Zhou, J. Cheng, Y. Chen, G. Hou, Y. Ding, Y. Li, Y. Zhao, X. Zhang, *J. Power Sources* **2021**, *485*, 229313.

[11] N. H. Tiep, Z. Ku, H. J. Fan, *Adv. Energy Mater.* **2016**, *6*, 1501420.

[12] S. Wang, H. Chen, J. Zhang, G. Xu, W. Chen, R. Xue, M. Zhang, Y. Li, Y. Li, *Adv. Mater.* **2019**, *31*, 1903691.

[13] N. J. Jeon, J. H. Noh, W. S. Yang, Y. C. Kim, S. Ryu, J. Seo, S. Il Seok, *Nature* **2015**, *517*, 476.

[14] G. Grancini, C. Roldán-Carmona, I. Zimmermann, E. Mosconi, X. Lee, D. Martineau, S. Narbey, F. Oswald, F. De Angelis, M. Graetzel, M. K. Nazeeruddin, *Nat. Commun.* **2017**, *8*, 15684.

[15] X. Li, Y. Meng, R. Liu, Z. Yang, Y. Zeng, Y. Yi, W. E. I. Sha, Y. Long, J. Yang, *Adv. Energy Mater.* **2021**, *n/a*, 2102844.

[16] M. Acik, S. B. Darling, *J. Mater. Chem. A* **2016**, *4*, 6185.

[17] S. Jeong, I. Lee, T.-S. Kim, J.-Y. Lee, *Adv. Mater. Interfaces* **2020**, *7*, 2001425.

[18] Y. Bai, Q. Dong, Y. Shao, Y. Deng, Q. Wang, L. Shen, D. Wang, W. Wei, J. Huang, *Nat. Commun.* **2016**, *7*, 12806.

[19] I. S. Yang, N. G. Park, *Adv. Funct. Mater.* **2021**, *31*, 2100396.

[20] B. Yang, J. Suo, F. Di Giacomo, S. Olthof, D. Bogachuk, Y. Kim, X. Sun, L. Wagner, F. Fu, S. M. Zakeeruddin, A. Hinsch, M. Grätzel, A. Di Carlo, A. Hagfeldt, *ACS Energy Lett.* **2021**, *6*, 3916.

[21] S. Ghosh, T. Singh, *Nano Energy* **2019**, *63*, 103828.

[22] S. Wang, Z. Li, Y. Zhang, X. Liu, J. Han, X. Li, Z. Liu, S. (Frank) Liu, W. C. H. Choy, *Adv. Funct. Mater.* **2019**, *29*, 1900417.

[23] X. X. Gao, B. Ding, H. Kanda, Z. Fei, W. Luo, Y. Zhang, N. Shibayama, A. Züttel, F. F. Tirani, R. Scopelliti, S. Kinge, B. Zhang, Y. Feng, P. J. Dyson, M. K. Nazeeruddin, *Cell Rep. Phys. Sci.* **2021**, *2*, 100475.

[24] D. Yang, X. Zhou, R. Yang, Z. Yang, W. Yu, X. Wang, C. Li, S. Liu, R. P. H. Chang, *Energy Environ. Sci.* **2016**, *9*, 3071.

[25] M. Li, C. Zhao, Z. K. Wang, C. C. Zhang, H. K. H. Lee, A. Pockett, J. Barbé, W. C. Tsoi, Y. G. Yang, M. J. Carnie, X. Y. Gao, W. X. Yang, J. R. Durrant, L. S. Liao, S. M. Jain, *Adv. Energy Mater.* **2018**, *8*, 1801509.

[26] P. Caprioglio, D. S. Cruz, S. Caicedo-Dávila, F. Zu, A. A. Sutanto, F. Peña-Camargo, L. Kegelmann, D. Meggiolaro, L. Gregori, C. M. Wolff, B. Stiller, L. Perdigón-Toro, H. Köbler, B. Li, E. Gutierrez-Partida, I. Lauermann, A. Abate, N. Koch, F. De Angelis, B. Rech, G. Grancini, D. Abou-Ras, M. K. Nazeeruddin, M. Stolterfoht, S. Albrecht, M. Antonietti, D. Neher, *Energy Environ. Sci.* **2021**, *14*, 4508.

[27] S. Bai, P. Da, C. Li, Z. Wang, Z. Yuan, F. Fu, M. Kawecki, X. Liu, N. Sakai, J. T. W. Wang, S. Huettner, S. Buecheler, M. Fahlman, F. Gao, H. J. Snaith, *Nature* **2019**, *571*, 245.

[28] Q. Ye, F. Ma, Y. Zhao, S. Yu, Z. Chu, P. Gao, X. Zhang, J. You, *Small* **2020**, *16*, 2005246.
[29] Y. Chen, M. He, J. Peng, Y. Sun, Z. Liang, *Adv. Sci.* **2016**, *3*, 1500392.
[30] T. A. Berhe, W. N. Su, C. H. Chen, C. J. Pan, J. H. Cheng, H. M. Chen, M. C. Tsai, L. Y. Chen, A. A. Dubale, B. J. Hwang, *Energy Environ. Sci.* **2016**, *9*, 323.
[31] J. A. Christians, P. A. Miranda Herrera, P. V. Kamat, *J. Am. Chem. Soc.* **2015**, *137*, 1530.
[32] T. Xu, L. Chen, Z. Guo, T. Ma, *Phys. Chem. Chem. Phys.* **2016**, *18*, 27026.
[33] G. E. Eperon, S. D. Stranks, C. Menelaou, M. B. Johnston, L. M. Herz, H. J. Snaith, *Energy Environ. Sci.* **2014**, *7*, 982.
[34] Z. Li, M. Yang, J. S. Park, S. H. Wei, J. J. Berry, K. Zhu, *Chem. Mater.* **2016**, *28*, 284.
[35] Z. Yao, W. Zhao, S. Liu, *J. Mater. Chem. A* **2021**, *9*, 11124.
[36] R. Chen, Y. Hui, B. Wu, Y. Wang, X. Huang, Z. Xu, P. Ruan, W. Zhang, F. Cheng, W. Zhang, J. Yin, J. Li, N. Zheng, *J. Mater. Chem. A* **2020**, *8*, 9597.
[37] B. Li, Y. Zhang, L. Fu, T. Yu, S. Zhou, L. Zhang, L. Yin, *Nat. Commun.* **2018**, *9*, 1076.
[38] J. J. van Franeker, K. H. Hendriks, B. J. Bruijnaers, M. W. G. M. Verhoeven, M. M. Wienk, R. A. J. Janssen, *Adv. Energy Mater.* **2017**, *7*, 1601822.
[39] L. Huang, Z. Hu, J. Xu, K. Zhang, J. Zhang, Y. Zhu, *Sol. Energy Mater. Sol. Cells* **2015**, *141*, 377.
[40] T. Leijtens, K. Bush, R. Cheacharoen, R. Beal, A. Bowring, M. D. McGehee, *J. Mater. Chem. A* **2017**, *5*, 11483.
[41] H. S. Kim, J. Y. Seo, N. G. Park, *ChemSusChem* **2016**, *9*, 2528.
[42] D. Wang, M. Wright, N. K. Elumalai, A. Uddin, *Sol. Energy Mater. Sol. Cells* **2016**, *147*, 255.
[43] T. Leijtens, G. E. Eperon, S. Pathak, A. Abate, M. M. Lee, H. J. Snaith, *Nat. Commun.* **2013**, *4*, 2885.
[44] J. Yang, B. D. Siempelkamp, E. Mosconi, F. De Angelis, T. L. Kelly, *Chem. Mater.* **2015**, *27*, 4229.
[45] Z. Hawash, L. K. Ono, S. R. Raga, M. V. Lee, Y. Qi, *Chem. Mater.* **2015**, *27*, 562.
[46] Q. Xue, M. Liu, Z. Li, L. Yan, Z. Hu, J. Zhou, W. Li, X. F. Jiang, B. Xu, F. Huang, Y. Li, H. L. Yip, Y. Cao, *Adv. Funct. Mater.* **2018**, *28*, 1707444.
[47] Y. Kato, L. K. Ono, M. V. Lee, S. Wang, S. R. Raga, Y. Qi, *Adv. Mater. Interfaces* **2015**, *2*, 1500195.
[48] K. Domanski, J. P. Correa-Baena, N. Mine, M. K. Nazeeruddin, A. Abate, M. Saliba, W. Tress, A. Hagfeldt, M. Grätzel, *ACS Nano* **2016**, *10*, 6306.
[49] E. Y. Muslih, A. K. M. Hasan, L. Wang, *Chem. Eng. J.* **2021**, *411*, 128461.
[50] M. Vasilopoulou, A. Fakharuddin, A. G. Coutsolelos, P. Falaras, P. Argitis, A. R. B. M. Yusoff, M. K. Nazeeruddin, *Chem. Soc. Rev.* **2020**, *49*, 4496.
[51] Y. H. Lin, N. Sakai, P. Da, J. Wu, H. C. Sansom, A. J. Ramadan, S. Mahesh, J. Liu, R. D. J. Oliver, J. Lim, L. Aspitarte, K. Sharma, P. K. Madhu, A. B. Morales-Vilches, P. K. Nayak, S. Bai, F. Gao, C. R. M. Grovenor, M. B. Johnston, J. G. Labram, J. R. Durrant, J. M. Ball, B. Wenger, B. Stannowski, H. J. Snaith, *Science* **2020**, *369*, 96.
[52] T. Niu, L. Chao, W. Gao, C. Ran, L. Song, Y. Chen, L. Fu, W. Huang, *ACS Energy Lett.* **2021**, *6*, 1453.
[53] X. Deng, L. Xie, S. Wang, C. Li, A. Wang, Y. Yuan, Z. Cao, *Chem. Eng. J.* **2020**, *398*, 125594.
[54] R. Xia, X. X. Gao, Y. Zhang, N. Drigo, V. I. E. Queloz, F. F. Tirani, R. Scopelliti, Z. Huang, X. Fang, S. Kinge, Z. Fei, C. Roldán-Carmona, M. K. Nazeeruddin, P. J. Dyson, *Adv. Mater.* **2020**, *32*, 2003801.
[55] X. Xia, J. Peng, Q. Wan, X. Wang, Z. Fan, J. Zhao, F. Li, *ACS Appl. Mater. Interfaces* **2021**, *13*, 17677.
[56] J. Wang, X. Ye, Y. Wang, Z. Wang, W. Wong, C. Li, *Electrochim. Acta* **2019**, *303*, 133.
[57] M. Salado, M. A. Fernández, J. P. Holgado, S. Kazim, M. K. Nazeeruddin, P. J. Dyson, S. Ahmad, *ChemSusChem* **2017**, *10*, 3846.
[58] D. Liu, Z. Shao, J. Gui, M. Chen, M. Liu, G. Cui, S. Pang, Y. Zhou, *Chem. Commun.* **2019**, *55*, 11059.
[59] S. Akin, E. Akman, S. Sonmezoglu, *Adv. Funct. Mater.* **2020**, *30*, 2002964.
[60] M. Shahiduzzaman, L. Wang, S. Fukaya, E. Y. Muslih, A. Kogo, M. Nakano, M. Karakawa, K. Takahashi, K. Tomita, J. M. Nunzi, T. Miyasaka, T. Taima, *ACS Appl. Mater. Interfaces* **2021**, *13*, 21194.
[61] M. Shahiduzzaman, K. Yamamoto, Y. Furumoto, T. Kuwabara, K. Takahashi, T. Taima, *RSC Adv.* **2015**, *5*, 77495.
[62] X. Zhu, M. Du, J. Feng, H. Wang, Z. Xu, L. Wang, S. Zuo, C. Wang, Z. Wang, C. Zhang, X. Ren, S. Priya, D. Yang, S. Liu, *Angew. Chem Int. Ed.* **2021**, *60*, 4238.
[63] L. Caliò, M. Salado, S. Kazim, S. Ahmad, *Joule* **2018**, *2*, 1800.
[64] N. Harindu Hemasiri, S. Kazim, L. Calio, S. Paek, M. Salado, G. Pozzi, L. Lezama, M. K. Nazeeruddin, S. Ahmad, *ACS Appl. Mater. Interfaces* **2020**, *12*, 9395.
[65] M. Salado, A. D. Jodlowski, C. Roldan-Carmona, G. de Miguel, S. Kazim, M. K. Nazeeruddin, S. Ahmad, *Nano Energy* **2018**, *50*, 220.
[66] X. Zhou, Y. Wang, C. Li, T. Wu, *Chem. Eng. J.* **2019**, *372*, 46.
[67] M. Li, Z.-K. Wang, M.-P. Zhuo, Y. Hu, K.-H. Hu, Q.-Q. Ye, S. M. Jain, Y.-G. Yang, X.-Y. Gao, L.-S. Liao, *Adv. Mater.* **2018**, *30*, 1800258.
[68] R. Xu, H. Dong, P. Li, X. Cao, H. Li, J. Li, Z. Wu, *ACS Appl. Mater. Interfaces* **2021**, *13*, 33218.
[69] L. Yang, X. Ma, X. Shang, D. Gao, C. Wang, M. Li, C. Chen, B. Zhang, S. Xu, S. Zheng, H. Song, *Sol. RRL* **2021**, *5*, 2100352.
[70] Z. Lin, Y. Su, R. Dai, G. Liu, J. Yang, W. Sheng, Y. Zhong, L. Tan, Y. Chen, *ACS Appl. Mater. Interfaces* **2021**, *13*, 15420.
[71] Y. Du, Q. Tian, X. Chang, J. Fang, X. Gu, X. He, X. Ren, K. Zhao, S. Liu, *Adv. Mater.* **2022**, 2106750.
[72] A. Wang, X. Deng, J. Wang, S. Wang, X. Niu, F. Hao, L. Ding, *Nano Energy* **2021**, *81*, 105631.
[73] R. Yin, K. Wang, S. Cui, B. Fan, J. Liu, Y. Gao, T. You, P. Yin, *ACS Appl. Energy Mater* **2021**, *4*, 9294.
[74] C. Luo, G. Li, L. Chen, J. Dong, M. Yu, C. Xu, Y. Yao, M. Wang, Q. Song, S. Zhang, *Sustain. Energy Fuels* **2020**, *4*, 3971.
[75] Y. Zhang, Z. Fei, P. Gao, Y. Lee, F. F. Tirani, R. Scopelliti, Y. Feng, P. J. Dyson, M. K. Nazeeruddin, *Adv. Mater.* **2017**, *29*, 1702157.
[76] Z. Zhang, T. Guo, H. Yuan, L. Yu, R. Zhao, Z. Deng, J. Zhang, X. Liu, Z. Hu, Y. Zhu, *ACS Appl. Mater. Interfaces* **2021**, *13*, 727.
[77] J. Y. Seo, T. Matsui, J. Luo, J. P. Correa-Baena, F. Giordano, M. Saliba, K. Schenk, A. Ummadisingu, K. Domanski, M. Hadadian, A. Hagfeldt, S. M. Zakeeruddin, U. Steiner, M. Grätzel, A. Abate, *Adv. Energy Mater.* **2016**, *6*, 1600767.
[78] J. Yang, W. Sheng, R. Li, L. Gong, Y. Li, L. Tan, Q. Lin, Y. Chen, *Adv. Energy Mater.* **2022**, 2103652.
[79] S. Wang, B. Yang, J. Han, Z. He, T. Li, Q. Cao, J. Yang, J. Suo, X. Li, Z. Liu, S. F. Liu, C. Tang, A. Hagfeldt, *Energy Environ. Sci.* **2020**, *13*, 5068.
[80] G. Li, Z. Su, M. Li, F. Yang, M. H. Aldamasy, J. Pascual, F. Yang, H. Liu, W. Zuo, D. Di Girolamo, Z. Iqbal, G. Nasti, A. Dallmann, X. Gao, Z. Wang, M. Saliba, A. Abate, *Adv. Energy Mater.* **2021**, *11*, 2101539.
[81] Y. Wang, L. Chao, T. Niu, D. Li, Q. Wei, H. Wu, J. Qiu, H. Lu, C. Ran, Q. Zhong, L. Song, G. Xing, Y. Xia, Y. Chen, P. Müller-Buschbaum, W. Huang, *Sol. RRL* **2021**, *5*, 2000582.
[82] J. Du, Y. Wang, Y. Zhang, G. Zhao, Y. Jia, X. Zhang, Y. Liu, *Phys. Status Solidi RRL* **2018**, *12*, 1800130.
[83] W. Zhang, X. Liu, B. He, Z. Gong, J. Zhu, Y. Ding, H. Chen, Q. Tang, *ACS Appl. Mater. Interfaces* **2020**, *12*, 4540.

Fei Wang received his master's degree in materials science and engineering from Shenzhen University in 2021. He was working as a research assistant in Prof. Hanlin Hu's group at the Hoffmann Institute of Advanced Materials, Shenzhen Polytechnic. He is currently a joint Ph.D. student of Wuhan University of Technology and the Hoffmann Institute of Advanced Materials. His research interests include ionic liquids engineering for perovskite solar cells and materials characterization based on X-ray scattering.

Chuang-Ye Ge received his Ph.D. degree in applied chemistry from Konkuk University in South Korea in 2020. He is currently working as a postdoctoral fellow in Prof. Hanlin Hu's group at the Hoffmann Institute of Advanced Materials, Shenzhen Polytechnic. His research interests include low-dimensional perovskite synthesis, scalable fabrication manufacturing, and flexible perovskite solar cells.

Dawei Duan received his master's degree in applied chemistry from Sumy National Agrarian University in Ukraine in 2021. He is currently working as a research assistant in Prof. Hanlin Hu's group at the Hoffmann Institute of Advanced Materials, Shenzhen Polytechnic. His research interests include high-quality quantum dots synthesis, ionic liquids engineering for perovskite photovoltaics, and slot-die coating for upscaling of perovskite solar cells.

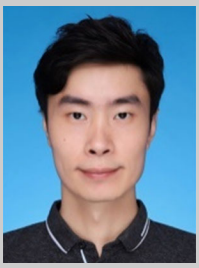

Haoran Lin received his bachelor's degree in chemistry from Peking University and his Ph.D. degree in chemistry from the Hong Kong University of Science and Technology. He then worked as a postdoctoral fellow in Prof. Biwu Ma's group at Florida State University. He is currently an associate professor at the Hoffmann Institute of Advanced Materials in Shenzhen Polytechnic, continuing his research on organic–inorganic hybrid materials and optoelectronic devices. He has published over 40 papers in high impact factors journals, with total over 8000 citations and an *h*-index of 28.

Liang Li received his B.Sc. from Shandong University and a Ph.D. degree in physics from the University of Bayreuth. He served as a staff scientist at the King Abdullah University of Science and Technology and New York University Abu Dhabi for 10 years. In 2021, he joined Sorbonne University Abu Dhabi as an assistant professor of physics. He is currently also affiliated with the Division of Science at New York University Abu Dhabi. His research focuses on smart materials, new energy-related materials, and quantum technologies.

Panče Naumov was educated and worked shortly at Ss. Cyril and Methodius University in Skopje, Macedonia. After acquiring his Ph.D. in chemistry and materials science from Tokyo Institute of Technology in 2004, he continued his research at the National Institute for Materials Science, Osaka University and Kyoto University in Japan. In 2007, he joined New York University, where he is now a tenured faculty in NYU's portal campus in Abu Dhabi, the UAE. The research in the Naumov Group is in the materials science domain, focusing on smart materials, crystallography, bioluminescence, and petroleomics.

Hanlin Hu obtained his Ph.D. degree from the Department of Materials Science and Engineering at King Abdullah University of Science and Technology in Saudi Arabia in 2015. After that, he carried out his post-doctoral research in Prof. Gang Li's group at the Hong Kong Polytechnic University. He is currently an associate professor at the Hoffmann Institute of Advanced Materials, Shenzhen Polytechnic. He has established the Synchrotron and Printable Electronic Devices Lab at HIAM equipped with in-house GIWAXS/GISAXS. He has published 50+ papers with an *h*-index of 21. His research focuses on printing thin-film solar cells, transistors, and synchrotron-based phase-transition studies.